Journal of Applied Polymer Science

The Effect of Surface Treatment on Graphite Nanoplatelets Used in Fiber reinforced Composites

Rafael J. Zaldivar, James P. Nokes, Hyun I. Kim
The Aerospace Corporation, Material Sciences Department, California
Correspondence to: R. J. Zaldivar (E-mail: rjz@aero.org)

ABSTRACT: Atmospheric plasma treatment (APT) was used to surface-activate graphite nanoplatelets (GnP) as well as highly graphitic P100 fibers used to manufacture composites. X-ray photoelectron spectroscopy showed an increase in the O/C ratio of the treated surfaces when using either CO or O_2 as the active gas, whereas CO exhibited less damage to the treated reinforcement carbon material. APT of P100 fibers resulted in a 75% increase in composite tensile strength when compared to composites using untreated fibers. Surface treatment of GnPs also resulted in GnP/epoxy composites with significantly higher glass transition temperatures (Tg's) and 50% higher flexural strengths than those with no surface treatment because of stronger particle-to-resin coupling, which was also evidenced by the fracture surfaces. The effect of GnP loading concentration and plasma treatment duration was also evaluated on the tensile strength of fiber-reinforced composites. The addition of untreated GnP filler resulted in a decrease in strength up to the 1% loading. However, higher loading conditions resulted in a 20% improvement because of GnP orientation effects. Fracture surfaces suggest that the fibers provided a mechanism for the GnPs to orient themselves parallel to the fiber axis, developing an oriented matrix microstructure that contributes to added crack deflection. Incorporating surface-treated GnPs in these composites resulted in tensile strengths that were as high as 50% stronger than the untreated systems for all loading conditions. Increased GnP-to-matrix bonding as well as enhanced orientation of the GnPs resulted in multifunctional composites with improved mechanical performance.
 J. Appl. Polym. Sci. **2014**, *131*, 39994.

KEYWORDS: composites; functionalization of polymers; nanotubes; graphene and fullerenes

Received 31 July 2013; accepted 22 September 2013
DOI: 10.1002/app.39994

INTRODUCTION

Graphite Nanoplatelets (GnPs) are nanocarbon particulates that are manufactured by the intercalation, exfoliation, and ball milling and of graphite.[1] These submicron materials have excellent mechanical and electrical properties similar to that of graphite.[2] They have been proposed as alternatives to fillers such as carbon black, metal particulates and more recently the extensively investigated single wall and multiwall carbon nanotubes at a fraction of the cost. Typically, traditional fillers such as carbon black and graphite that are incorporated into composites for electrical and thermal improvements require high percolation threshold levels (15–40 wt %) to achieve conductivy.[3] However, these higher loading levels are usually associated with a degradation of the mechanical properties of the neat resin.[4] On the other hand, GnPs require percolation levels that are typically an order of magnitude lower than traditional conductive fillers because of their unique aspect ratio.

Even though these reinforcements have excellent properties, the composite properties are usually limited by the weak interfaces between the graphitic platelets and the polymer matrix material. The same highly oriented, basal plane structures in these materials that provide many of the desired properties sought also result in poor wetting and reduced molecular interaction with conventional resins. Most highly graphitic materials have very few available surface chemical groups by which they bond to the surrounding matrix. Increasing the chemical activity on the surface of these nanographitic particulates has been shown to enhance wetting and potentially chemical bonding. Some techniques that have been used to improve this coupling with limited success are acid treatments, UV exposure, ozone treatment, and vacuum plasma treatments.[5,6] However, they are also associated with varying degrees of damage to the treated material. Oxygen gas atmospheric plasma treatment (APT) is a relatively new processing technique that has been used to clean and chemically modify the surface of carbon materials.[7] This treatment is performed at low temperatures and is typically constrained to the outermost nanometers, reducing the degree of material degradation. This treatment can also be performed using a wide array of active gases, depending on the functional groups desired on the surface being treated. APT using carbon monoxide gas has been shown to increase surface oxygen

content and improve wetting of carbon materials, while minimizing oxidative degradation.[8]

Though significant improvements in mechanical and thermal properties have been achieved when manufacturing GnP/resin composites, the full potential of these composites requires improved orientation and bonding of the filler. We believe that the use of highly graphitic fibers could provide a template for the GnP particles to form a networked orientation. Therefore, the synergy of using both reinforcements when manufacturing GnP loaded/carbon fiber composites will be explored. In this investigation, we will evaluate the effect of APT when using either CO or O_2 as the active gas on GnPs prior to composite manufacture. XPS will be used to evaluate changes to the surface chemistry of the GnPs with plasma treatments. A number of unidirectional carbon fiber composites will be manufactured using different GnPs loading concentrations. Both fiber-reinforced and GnP filled neat resin composites will be mechanically tested and compared to the untreated system to evaluate changes to mechanical performance. Composite fracture surfaces will also be analyzed to identify how microstructural variations as a result of APT may affect the performance.

EXPERIMENTAL

Graphite Nanoplatelets

Expanded graphite GnPs were used in this study. The specimens were obtained from XG Sciences and are designated M5. The number relates to the lateral size of the particulates, in microns. In order to disperse the GnPs, a 70 : 30 ethanol/THF mixture was utilized. A previous report discusses the process criteria in greater detail.[9] Five grams of solvent was used to dissolve 0.10 g of GnPs. The solvent was added to glass vial containing the GnPs and vigorously stirred with a glass rod for 5 minutes. Disperbyk 2150, a commercial dispersing agent was used in our formulations and provided by BYK Cheme. The concentration used was 0.01 wt %. The solution was then placed in an ultrasonic bath (45 kHz) for 55 minutes at room temperature until the large agglomerations were broken up. A high intensity tip sonicator (750 W, 20 kHz) was used to further dissociate any of the remaining particles in solution.

Four grams of Huntsman's Tactix 123 Epoxy was then heated to 120°C in aluminum casting plates. The GnP solution was added to the melted monomer and stirred for 15 minutes. The solution was allowed to degas until most of the solvent appeared to evaporate. The Aradur 5200 hardener (1.0 g) was then added to the solution and stirred for 25 additional minutes. Further heat treatment to 135°C allows the complete removal of gas bubbles from the solution. Once the solution appears void free, it is then placed in a drying oven at 120°C for 16 hours. The specimens are then HT to 160°C for 2 hours and cooled. Once cooled the cast resin pucks are removed from the aluminum pans and placed in a vacuum oven and HT to 180°C for a final 3 hours.

For the manufacture of unidirectional tows, a specified rack was used to hold and align unidirectional tows in the vertical position. Five grams of Aradur epoxy and hardener was added into the solvated solution of GnPs. The solution was stirred for 10 minutes and then used to infiltrate the tows. Solvent was allowed to dry and the entire rack and impregnated fibers were then cured, as previously described for the neat resin pucks. After cure, the tows were cut and trimmed for mechanical testing.

Plasma Treatment of Powders

A Surfx Technologies AtomFlo-400 atmospheric plasma unit was used to plasma treat all of our powdered specimens. The control unit uses helium gas as the carrier and oxygen as the active gas. All gases are of 99.9% purity. The plasma wand (Surfx PS02129) utilized a 25-mm linear beam. Plasma conditions were fixed at 100 W of radio frequency (13.56 MHz) power, 0.450 L/min of oxygen as the active gas, and 30 L/min of helium as the carrier gas. The treatment conditions when using carbon monoxide (CO) as the active gas were 110 W of RF power, 0.400 L/min of CO, and 30 L/min of helium. During treatment, the samples were placed on a stationary stage and a robotic arm holding the plasma head was scanned at a constant rate across the specimen face. The robotic arm has a lateral scan rate of 24.5 mm/s. The working distance was held fixed at 1.0 mm from the screen of the specimen holder. Further details are described elsewhere.[7]

A specially designed holder was used to treat GnPs powders. The holder was approximately 4.40 cm in length × 1.90 cm wide, and 0.25 cm deep. About 0.05 g of GnP powder was placed in the holder and a 400 mesh, 0.06 cm stainless steel screen was placed above the cavity. A windowpane support frame was then mechanically screwed onto the screen face to hold the powders in place. The screen allows the afterglow gases to flow onto the powder without causing loss of material. After 10 passes, the windowpane and screen were removed and the powder was recut and stirred to ensure additional areas would be exposed with further treatment. The lengths of duration (passes) for this study were 20, 40, and 60 passes.

The unsized carbon fibers (Amoco P100) described in this investigation were equally spaced (5 cm apart) and wrapped on a 30.5 cm × 30.5 cm aluminum frame that was held vertically. The two ends were adhered to the frame using a room temperature cured epoxy to prevent movement during the APT process. The plasma head was manually scanned at approximately 24.5 mm/s across the surfaces of the fibers for a total of six linear passes. The distance between the plasma head and the fibers was approximately 1 mm for both CO and O_2 treatment conditions. The plasma treatment was performed using the conditions previously described.

Dynamic Mechanical Analysis

A TA Instruments DMA Analyzer was used for all testing. The samples were scanned from room temperature to 300°C at a heating rate of 10°C /min. The samples were tested in a single cantilever mode at a frequency of 1 Hz and a maximum strain of 20 μm. The glass transition temperature (Tg) was identified as the maximum in loss modulus.

X-Ray Photoelectron Spectroscopy

X-ray photoelectron spectroscopy (XPS) system (SSI) using Al Kα source was used for surface chemical analysis as a function of plasma treatment for the treated GnP particles. Analyzer pass energies of

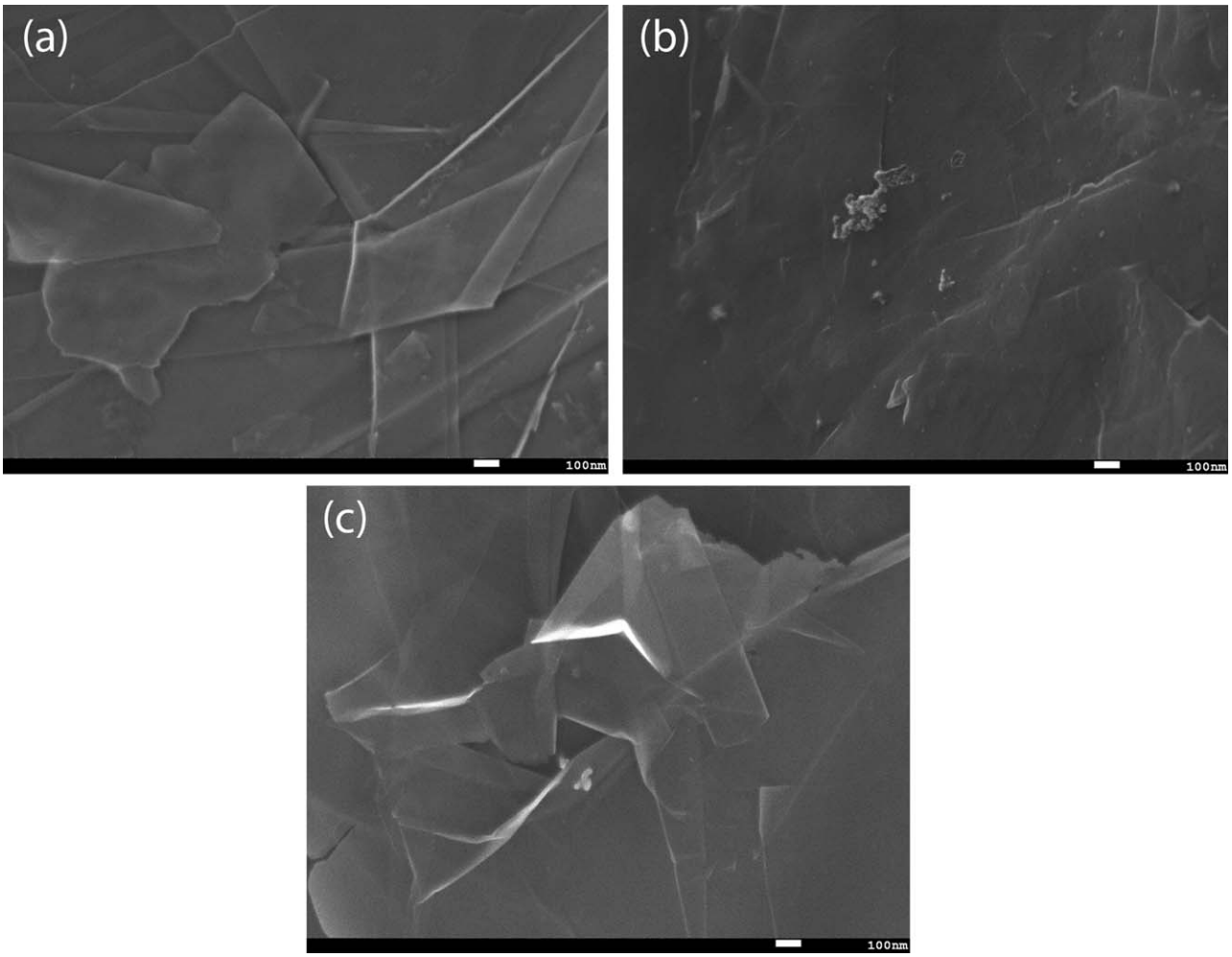

Figure 1. Scanning electron micrograph showing GNP platelets (a) as–is (b) CO treated (c) O_2 treated

150 and 50 eV were used for wide scans and high-resolution spectra, respectively. The XPS analysis chamber was pumped by an ion pump and had a base pressure of 1×10^{-10} Torr.

Raman Spectroscopy

Raman spectroscopy was used to characterize the molecular morphology of the GnPs used in this study, pre- and post-plasma treatment. Confocal Raman spectra were acquired with a Renishaw in via spectrometer equipped with a 514 nm laser and a 100× objective.

Three-Point Bend Testing

An Instron 1050 miniaturized frame with a 445-N load cell was used for all flexural tests of cast resin specimens. The flexural properties of the doped and undoped neat resin specimens were performed according to ASTM standard D790-96.[10] The molded specimens were cut into 7.0 mm wide × 25.4 mm long × 5.0 mm thick samples, which were subjected to a bending with a support span of 12.5 mm at a constant crosshead speed of 10 mm/min. The specimens were cut with a diamond blade.

Tensile Testing

Both, unidirectional P100 epoxy composites and GnP-filled epoxy P100 composites were tabbed and mounted with 0.317-cm card stock. The gauge length for all test specimens was maintained at 5.05 cm. All tensile strength values were obtained using a Universal Testing Machine and following ASTM D4018.[11] A 500-N load cell with a load ramp rate of 0.1/min. was used. Ten samples were tested for each condition described.

RESULTS AND DISCUSSION

A scanning electron micrograph showing the microstructure of typical untreated GnP investigated in this study is shown in Figure 1. A comparable photo is shown after APT, using either carbon monoxide [Figure 1(b)] or oxygen [Figure 1(c)] as the active gas. As shown in Figure 1(a), the structure is composed on thin graphite platelets that are stacked upon each other. The CO-treated specimen shows less microstructural detail because of the deposition of a thin nanoscaled highly oxidized coating that grows as a function of treatment time. Details regarding the structure of the coating have been described in a previous publication.[12] On the other hand, the microstructure of the oxygen treated GnP specimen appears similar in detail to the untreated specimen. At longer treatment times, localized pitting because of oxidation has been observed.

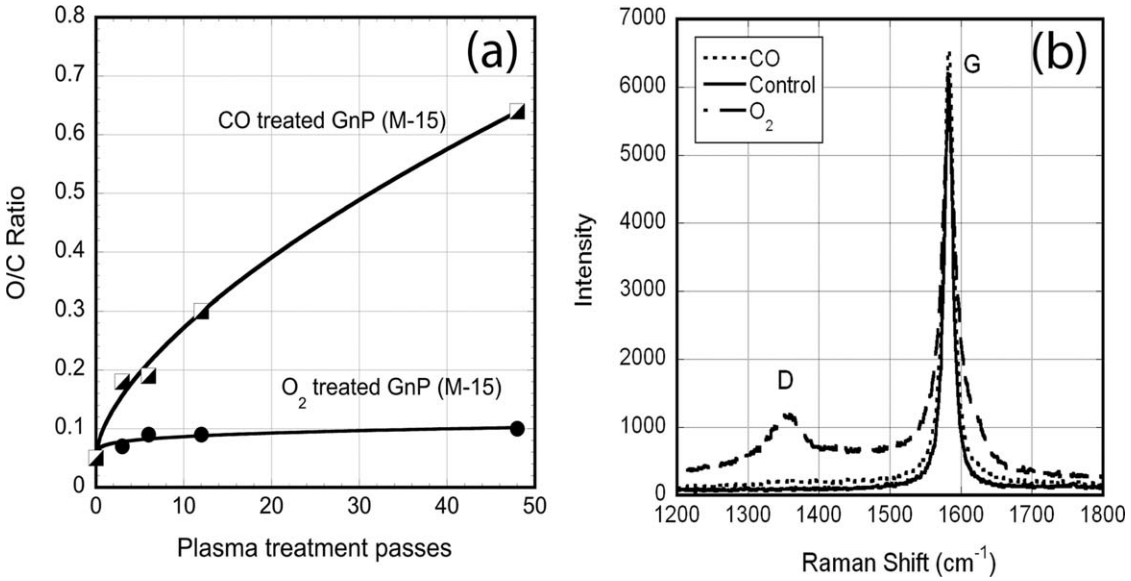

Figure 2. XPS of GnP packed powder as a function of APP treatment (a) O/C ratio for both CO and O_2 treated GnPs (b) Raman spectra for control, CO and O_2 treated GnP

The GnP specimens were also evaluated as a function of treatment passes and analyzed using both XPS and Raman microscopy. As shown in Figure 2(a), the oxygen : carbon ratio increases to approximately 0.1, which is in line with treatments reported in the literature for carbon nanomaterials exposed to oxygen plasma. This corresponds to the maximum oxygen uptake levels for highly graphitic materials. The incorporation of oxygen is limited to the available sites at the edges of the basal planes and/or defect sites on the outer surfaces of the carbon material. The CO treated specimens also increase with treatment passes but have a significantly higher O/C ratio, which approaches 0.6. For this case, a fair portion of the oxygen content is attributed to a highly oxidized nano-scaled coating that is deposited and strongly adhered onto the surface of the basal planes of the carbon substrate. High-resolution XPS spectra identified the primary functional groups formed after oxygen plasma treatment as alkoxy groups.[12]

The Raman spectra in Figure 2(b), show the characteristic graphitic, G, and disordered peak, D, for our GnP material. Studies have shown that as the disorder (D) of the carbon lattice increases, the relative ratio of the D to G peaks also increases.[13] An increase in disorder can reduce electrical as well as mechanical properties; therefore surface treatment should be performed in a manner to minimize damage. As shown, the as-received material appears quite well ordered and graphitic in nature. However, as the treatment duration increases, oxygen plasma treatment shows a corresponding increase in the intensity of the disordered peak. On the other hand, the carbon monoxide plasma treated specimens show little to no increase or change in the disordered state of the carbon.

For the case of the oxygen plasma treatment, the increase in the D peak intensity implies degradation or at the very least a disruption of the lattice. Previous studies utilizing scanning tunneling microscopy (STM) of highly oriented pyrolytic graphite (HOPG) that were treated using identical oxygen plasma conditions showed extensive nanometer scaled voids distributed throughout the outer surface of the samples.[14] This type of degradation correlates with increases in the D peak intensity. However, STM of CO plasma-treated specimens showed relatively the same surface step features of the untreated specimen without any indication of damage consistent with our Raman results. High-resolution STM scans of the CO coating exhibits a lattice structure similar to the HOPG substrate, whereas Auger spectroscopy showed oxygen evenly distributed throughout the surface of the specimen. Increases in O/C levels of the CO treated specimens were achieved by deposition of a highly order oxidized nanometer-scaled coating, which appears to have no negative impact on the structure of the substrate, as corroborated by negligible changes in the intensity of the D peak with exposure.[14]

In order to evaluate the magnitude of contributions to bonding from APT, untreated P100 pitch based carbon fibers were APT treated and manufactured into composites. The fibers are highly graphitic and representative of the unreactive surfaces of the GnPs, yet provide an easier mechanism to evaluate improvements in mechanical performance as a function of APT exposure. The samples were tensile tested to evaluate any changes in strength because of either improvements or reductions in stress transfer.

Table I shows the effect of APT on the tensile strength of P100/epoxy composites using two different active gases. The changes were observed for exposure durations ranging from 0 to 12 passes. As shown, both plasma gas treatments show increases in strength with APT treatment. The strength of the CO-treated specimens increase continuously after 12 passes of exposure by as much as 49%. The oxygen-treated specimens show an even greater degree of improvement with a 76% increase in tensile strength after only six passes. Further duration (passes) for the oxygen condition results in a decrease in tensile strength possibly because of excessive oxidation.

Table I. Normalized Tensile Strength of APT High Modulus P100 Pitch-based Carbon Fiber Composites

Passes	Tensile Strength of untreated fiber composite (Control) **(MPa)**	Tensile Strength of CO treated fiber composite **(MPa)**	Tensile Strength Improvement **(%)**	Tensile Strength of O_2 treated fiber composite **(MPa)**	Tensile Strength Improvement **(%)**
0	1317 ± 65				
1		1538 ± 75	+17%	1807 ± 122	+37%
3		1607 ± 85	+22%	2076 ± 78	+58%
6		1827 ± 102	+39%	2324 ± 146	+76%
12		1965 ± 83	+49%	2000 ± 95	+52%

Figure 3 shows the typical fracture surfaces of the P100/epoxy composite specimens investigated in this study. The control specimens [Figure 3(a)] show a high degree of fiber-to-matrix decoupling because of matrix shrinkage. As the bond is relatively weak at the fiber matrix interface, resin shrinkage leads to a fairly high degree of debonding resulting in poor stress transfer and lower tensile strengths. On the other hand, both the CO and oxygen plasma-treated specimens appear to couple more agressively to the resin than the control specimens. This improved interfacial bonding translates into higher tensile strengths as well as less interface debonding. The interface bond strength has increased sufficiently to shift the fracture into the highly oriented pleat-like structures within the fiber. This improvement may be a combination of improved wetting, mechanical interlocking, as well as chemical bonding contributions. It is difficult to exclude any of these contributions as they occur simulataneously. However, as the CO treatments provide less of an overall improvement with a correspondingly higher oxygen incorporation, mechanical interlocking cannot be overlooked as a primary contributor to the strength increase. The decreases observed at higher exposure conditions for the oxygen condition, however, emphasize the careful balance that must be maintained between the formation of oxygen functional groups to promote chemical bonding with the potential damage associated with oxygen degradation. APT of graphitic fillers using either O_2 and CO appear advantageous in improving composite properties when optimized with the proper conditions.

GnPs were then surface treated with APT using either CO or oxygen as the active gas. The treatment was performed as a function of duration (passes) for the two loading conditions. The treated GnPs were then incorporated into resin composites to evaluate changes to both thermal and mechanical properties. Table II shows a compilation of the glass transition temperature (Tg) for GnPs-treated composites. The Tg provides an indication of the solid to rubber transition for a given polymer system. The value is primarily dependent on the chemical structure as well as the amount of crosslinking a polymer has undergone after a specified degree of cure. The Tg of untreated GnP/epoxy composites at 0.5 and 1.0 wt % loading condition is 188°C and 182°C, respectively. Increasing the concentration of untreated GnPs decreases the Tg for this case. Decreases in Tg have been attributed to increased particle clustering, which may decrease the opportunity for GnP to polymer bonding when approaching the 1% loading condition.

O_2-APT of GnPs resulted in composites with higher Tg's than composites manufactured with untreated GnP fillers (Table II). Tg's for both the 0.5% and 1% composite specimens increased to as high as 198°C after 60 passes of APT, maintaining fixed concentrations. These increases in Tg are substantial and suggest that the oxygen functional groups formed on the GnP surfaces are chemically reacting with the surrounding matrix material, effectively acting as additional crosslinks. The CO-treated specimens also show an increase in Tg with treatment exposure, however, to a lesser degree. A maximum Tg of 191°C was observed for the 0.5% GnP/epoxy composite after 60 passes, from 188°C. The 1% CO-treated composite showed a maximum increase to 190°C, but showed a larger change in Tg possibly because of better distribution once treated than the untreated system. This suggests that APT improves particle-to-matrix coupling, which is encouraging and in line with our objective.

Specimens were then flexurally tested to evaluate changes to mechanical performance. Table III shows the flexural strengths for both concentrations of composites fabricated as a function of APT exposure conditions. As shown for the unmodified GnPs (control) composites, the flexural strength is approximately 96.5 MPa for the M5 0.5 wt % concentration specimens. The 1.0 wt % loading concentrations increases to 117 MPa, accounting for only an increase of approximately 25% for a doubling in concentration.

This limited improvement is possibly because of less efficient distribution at higher loading. However, upon exposure to APT with oxygen, both concentrations show considerable increases in strength. The flexural strength increases by 60% for the 0.5 wt % composites over that of the untreated GnP composites. This also trends with the Tg increases observed for the APT-treated GnP composites. The higher loading specimen shows similar increases, though more limited. These types of increases are believed to be a result of improved bonding at the particle to epoxy resin interface. The oxygen functional groups formed on the surface of the GnPs improve wetting of the resin as well as promote chemical bonding at the interface. Figure 4 shows the fracture surfaces of both APT and un-treated GnP composites. The specimen with no APT has a high degree of GnPs protruding from the surface, suggesting poor bonding. On the other hand, the plasma-treated specimen's fracture surface show very few indications of platelets extended above the fracture surface

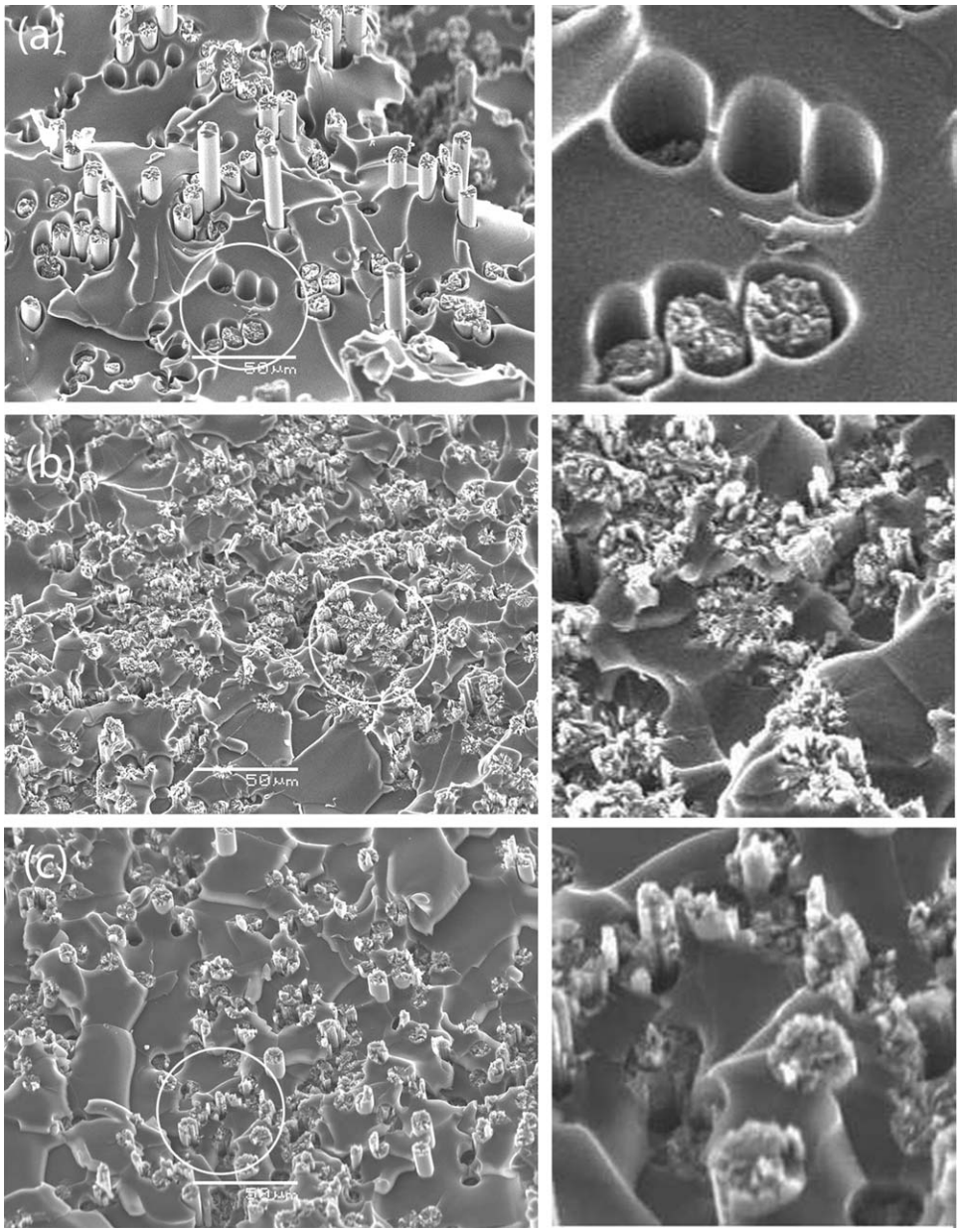

Figure 3. Fracture surface of composites with APT surface modified fibers (a) control, no APT (b) oxygen gas (c) carbon monoxide gas

[Figure 4(b)]. This fracture behavior is consistent with stronger particle-to-matrix coupling observed after APT, which supports the increases in flexural strength described earlier as well as the results for the APT-treated fibers. The CO-treated GnP composite specimens also show improvement with APT, yet to a lesser degree. This trends with the more gradual shifts in Tg observed for the CO-treated GnP composites in comparison to the O_2-treated composites.

Table II. Glass Transition Temperature using DMA for Composites Manufactured with O2 and CO-treated GnPs

Gas type	GnP Concentration (wt.%)	Control Tg (°C)	APP (20 pass) Tg (°C)	APP (40 pass) Tg (°C)	APP (60 pass) Tg (°C)
O_2	0.5	188	189	195	197
O_2	1.0	182	189	195	198
CO	0.5	188	189	190	191
CO	1.0	182	187	190	190

Table III. Flexural Strength of GnP/Epoxy Composites as a Function of GnP APT Exposure

			Flexural strength(MPa)			
GnP Filler	APT gas	Weight (%)	Control	20 APP	40 APP	60 APP
M5	O_2	0.5	96.5 ± 6.8	125.5 ± 8.9	151.7± 6.8	144.8 ± 4.8
	O_2	1.0	117.0 ± 5.5	137.2 ± 4.1	140.0 ± 7.6	133.8 ± 6.2
	CO	0.5	96.5 ± 6.8	110.0 ± 4.1	120.6 ± 6.2	128.2 ± 7.5
	CO	1.0	117.0 ± 5.5	118.6 ± 8.3	127.5 ± 5.5	123.4 ± 4.8

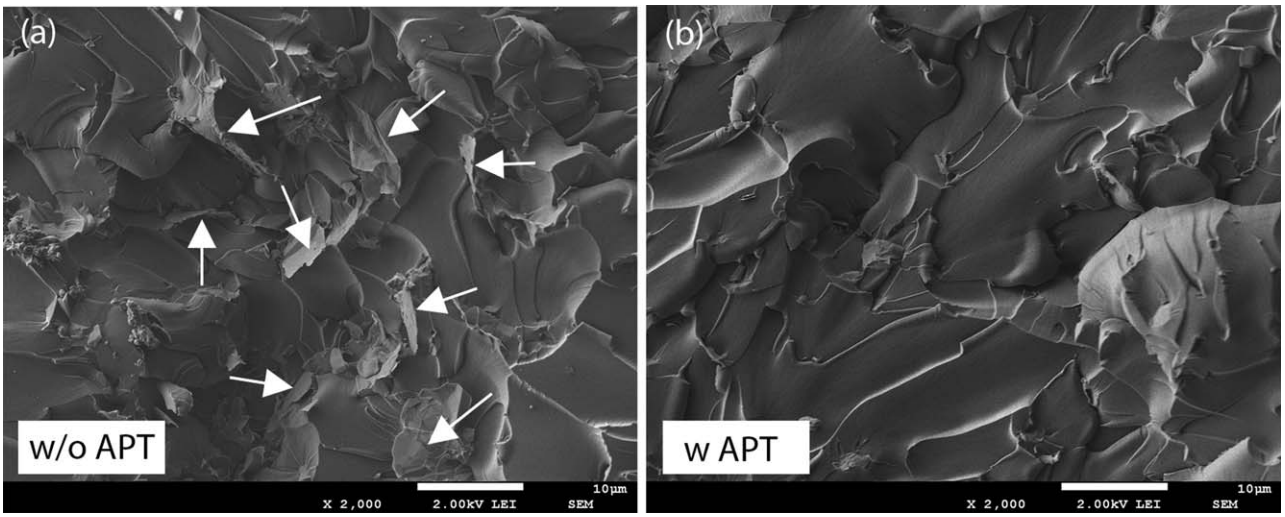

Figure 4. The effect of plasma treatment on the fracture behavior of GnP/epoxy composites. (a) w/o plasma treatment (b) w/ plasma treatment

Fiber/GnP-reinforced hybrid epoxy composites were then manufactured using a set concentration (0.5 wt %) of GnPs. A control specimen with untreated GnPs was used to make one set of composites, a second set with oxygen plasma-treated GnPs, and a third with 0.5 wt % CO-treated GnPs. Figure 5 shows a graph that exhibits the trend in mechanical performance with treatment condition. The graph is normalized to the tensile strength of the composite with no addition of GnPs. As shown, the addition of untreated 0.5 wt % GnPs to the composite causes a decrease or degradation in tensile strength. Approximately 25% of the initial strength is reduced because of the addition of the filler. Similar to other conventional fillers, the addition of the poorly bonded GnPs serve as defects that decrease the strength at the expense of an increase in conductivity. This is especially the case when the GnPs are random or lie perpendicular to the direction of the applied stress as many of the platelets are not completely exfoliated. However, if the particles are treated with CO prior to incorporation, the composite regains most of the initial unmodified tensile strength because of an increase in interfacial bond strength. The use of oxygen APT further increases and surpasses the tensile strength of the untreated material emphasizing how critical the interfacial bond strength is to final composite properties.

Figure 6 shows the tensile strength of these hybrid composites as a function of loading concentration. The properties shown are for the untreated GnP composites, CO-treated GnP composites, and O_2-treated GnP composites as a function of concentration. Only the GnPs were surface treated, the fibers were left intact to primarily emphasize the contributions from the addition of GnPs. As shown for the untreated GnPs (control) hybrid composites, the addition of GnPs causes a decrease in strength with increasing loading concentration up to 1.0% loading. Further

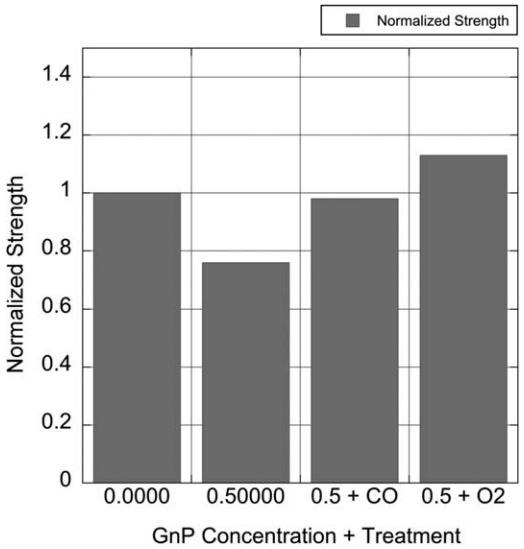

Figure 5. Graph showing effect of adding GnPs to tensile strength of Unidirectional Fiber reinforced epoxy composite.

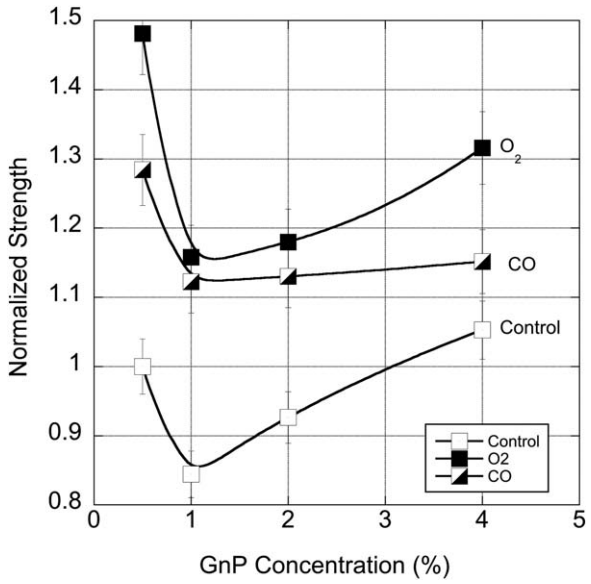

Figure 6. Normalized tensile strength of unidirectional hybrid composite manufactured using (a) control, unmodified GnPs (b) CO plasma treated GnPs (c) oxygen plasma treated GnPs

increases in loading concentration increase the tensile strength up to the 4 wt % level. Figures 7(a–d) show the fracture surfaces of the unmodified GnP/P100 epoxy composites. The matrix system with no GnP shows a featureless glass-like fracture surface with the highest strength. The strength is primarily dominated by the strength of the fiber and the efficiency at the fiber–matrix interface. The addition of GnPs to the matrix causes a reduction in tensile strength for all cases tested as the weakly bonded GnP platelets appear to behave as starter cracks. A load applied to the weak interface at the GnP-to-epoxy interface leads to premature failure. The addition of GnPs at low concentrations results in a matrix with randomly oriented platelets. However, as the concentration increases the platelets appear to orient themselves with respect to the fibers as shown in the fracture surface in Figure 7(d). This orientation of the GnP parallel to the fiber is much less prone to crack propagation than perpendicular to it. In addition, the improved orientation can deflect cracks and enhance the toughness of the composite.

For the oxygen plasma-treated GnP/fiber epoxy composite, the overall general trend of the tensile strength behavior with loading concentration is similar to the unmodified system. However,

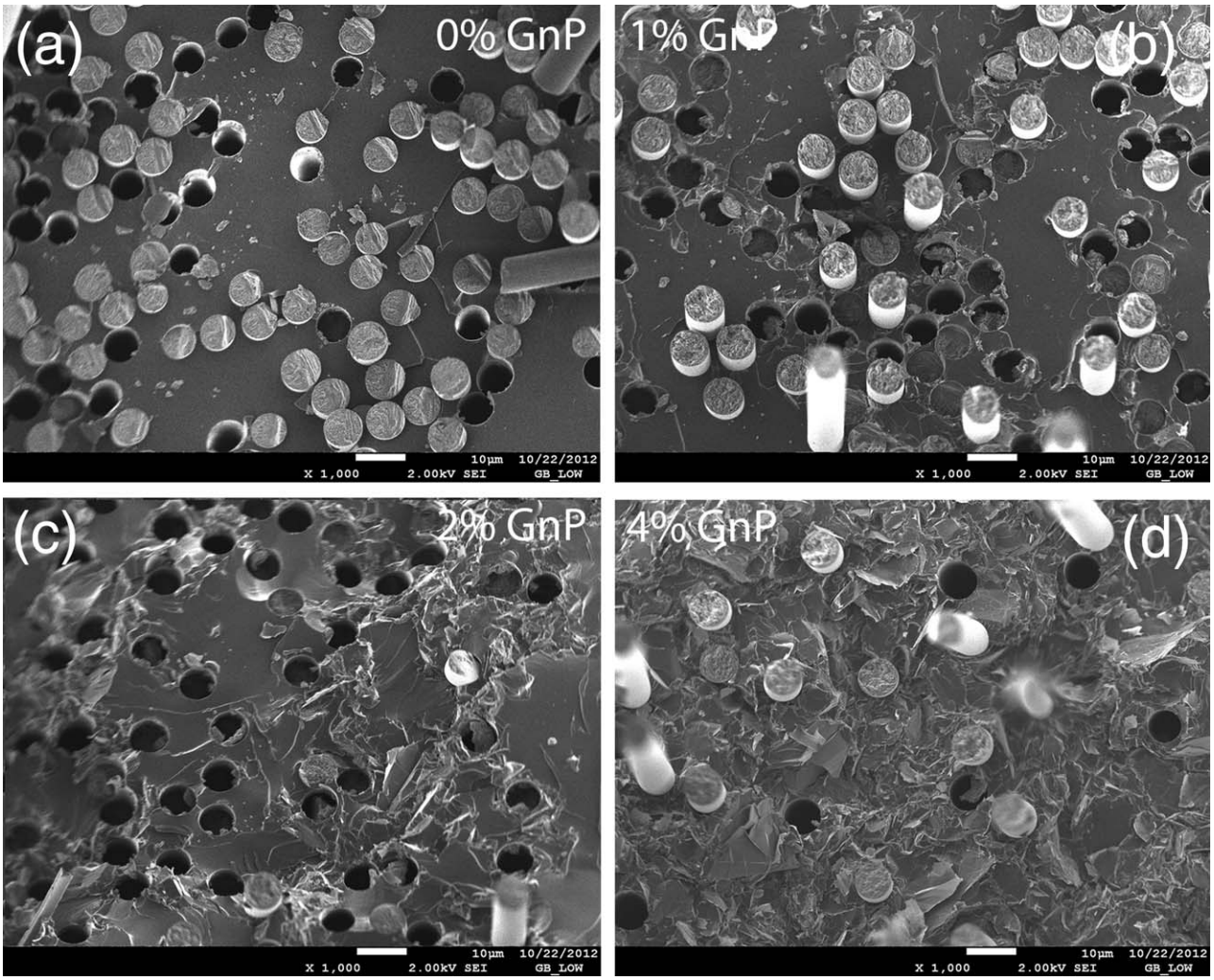

Figure 7. Fracture surface of GnP/P100 epoxy composite as a function of loading concentration (a) 0% GnP (b) 1% GnP (c) 2% GnP (d) 4% GnP

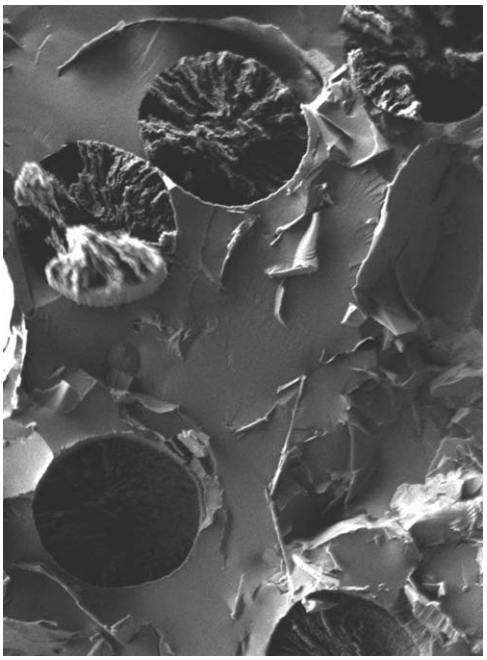

Figure 8. High magnification micrograph showing orientation of GnP platelets distributed in the surrounding matrix of the P100/GnP epoxy composites.

the strong GnP-to-epoxy matrix bonding results in a significant upward shift in the tensile strength profile as a function of GnP loading concentration. Increases approaching 50% were achieved over untreated GnPs. The CO-treated composite tensile strengths also show significant improvements, but to a lesser degree, which is in line with the reduced interfacial bond strength and Tg improvements reported previously for our CO-treated GnP epoxy composites.

The composite microstructures shown in Figure 7(d) (high loading level) and Figure 8 are similar to the lamellar-type matrix microstructures observed in carbon–carbon composites. During the graphitization of both phenolic and pitch-based matrices, there is an increase in the lamellar orientation of the matrix material parallel to the fiber. This structure is composed of graphitic basal planes parallel to the fiber direction. In resin-based composites, this orientation is typically a result of stress graphitization, whereas in pitch-based matrices the orientation is initially formed during the liquid crystalline mesophase transformation.15 The microstructure of the GnP filled matrix exhibits the same general orientation of this graphitic material in proximity to the fiber–matrix interface. This increased orientation of localized graphitic material has been shown to enhance mechanical properties by promoting crack deflection and blunting. Though the extent of localized graphitization is more extensive along the length of fibers in C/C composites, the addition of nanoscaled GnPs provides a pseudo-anisotropic microstructure in the matrix that appears to enhance mechanical performance in a similar manner, especially when well bonded. This increased particle-to-matrix bonding as well as enhanced orientation of the GnPs results in composites with improved mechanical performance. Optimizing surface treatment to enhance GnP distribution and bonding is the first step to manufacturing these composites as low cost alternatives for dual use applications.[16]

CONCLUSIONS

1. APT of GnPs using either CO or O_2 as the active gas increased the surface oxygen/carbon ratio. Both surfaces exhibit an increase in alkoxy functional groups with treatment. However, CO-treated samples exhibit less damage than the oxygen-treated GnP specimens.
2. Surface treatment of high modulus graphitic fibers significantly improved the composite tensile strength because of an enhancement in stress transfer using both CO and oxygen as the active gas. An increase of 76% and 49% in tensile strength was realized using oxygen and carbon monoxide, respectively. Fracture surfaces indicated improvements in bonding when compared to composites manufactured with untreated fibers that typically decoupled during cure. This shows that our APT conditions promote chemical bonding on highly graphitic materials resulting in improvements to mechanical performance.
3. Surface treatment of GnPs with both gases also resulted in increases in the Tg and flexural strengths of their composites. Improvements as high as 50% increase in flexural strength and a 10°C increase in Tg were realized. These increases are because of improvements in the GnP-to-epoxy bonding. Fracture surfaces of these composites corroborated improved bonding with treatment.
4. Hybrid high modulus fiber composites infiltrated with untreated GnPs exhibited an initial decrease in strength with loading. This 25–30% decrease is characteristic of weakly bonded fillers that behave as starter cracks. However, further increases in GnP concentration resulted in an increase in tensile strength because of an improved alignment of the GnPs, parallel to fiber axis.
5. Oxygen plasma treatment of GnPs used in these hybrid composites demonstrated further increases in mechanical performance using both gases. Increases in tensile strength approaching 50% were achieved over untreated composites. The CO-treated tensile strength of the hybrid composites also shows significant improvements, but to a lesser degree, which is in line with magnitude of interfacial bond strength gains described previously when added to neat resins.
6. Increased GnP-to-matrix bonding as well as enhanced orientation of the GnPs resulted in composites with improved mechanical performance, while providing a low cost potential alternative for multifunctional applications.

We would like to thank The Aerospace Corporation's Independent Research and Development program for their support.

REFERENCES

1. Kim, H.; Abdala, A. A.; Macosko, C. W. *Macromolecules* **2010**, *43*, 6515.
2. Potts J. R.; Dreyer, D. R.; Bielawski, C. W.; Ruoff, R. S. *Polymer* **2011**, *52*, 5.
3. Chen, G. H.; Wu, D. J.; Weng, W.; Yan, W. L. *J. Appl. Polym. Sci.* **2001**, *82*, 2506.

4. Xu, Y.; Chung, D. D. L.; Mroz, C. *Compos. Part A Appl. Sci. Manuf.* **2001**, *32*, 1749.
5. Li, J.; Sham, M.; Kim, J.; Marom, G. *Compos. Sci. Technol.* **2007**, *67*, 296.
6. Su, Q.; Pang, S.; Alijani, V.; Li, C.; Feng, X.; Mullen, K. *Adv. Mater.* **2009**, *21*, 3191.
7. Zaldivar, R. J.; Kim, H.; Steckel, G. L.; Morgan, B.; Nokes, J. P. *J. Compos. Mater.* **2010**, *44*, 2, 137.
8. Zaldivar, R. J.; Kim, H.; Steckel, G. L.; Morgan, B.; Nokes, J. P. *J. Compos. Mater.* **2010**, *44*, 12, 1435.
9. Zaldivar, R. J.; Adams, P. M.; Kim, H.; Patel, D. N.; Steckel, G. L.; Nokes, J. P. ATR 2013(8433-00)-1, The Aerospace Corporation, **2013**.
10. ASTM D790-10, Standard test methods for flexural properties of unreinforced plastics and electrical insulating materials, American Society for Testing and Materials Intl., West Conshoken, PA, USA, **2012**.
11. ASTM D4018, Properties of Continuous Filament Carbon and Graphite Fiber Tows, American Society for Testing and Materials Intl., West Conshoken, PA, USA, **2009**.
12. Zaldivar, R. J.; Adams, P. M.; Nokes, J. P.; Kim, H. I. *J. Vac. Sci. Technol. B* **2012**, *30*, 03D107.
13. Dresselhaus, M. J.; Jorio, A.; Hofmann, M.; Dresselhaus, G.; Saito, R. *Nano Lett.* **2010**, *10*, 751.
14. Zaldivar, R. J.; Nokes, J.P.; Adams, P.M.; Hammoud, K.; Kim, H.I. *Carbon* **2012**, *50*, 2966.
15. Zaldivar, R. J.; Rellick, G. S. *Carbon* **1991**, *29*, 8, 1155.
16. Loomis, J.; Fan, X.; Khosravi, F.; Xu, P.; Fletcher, M.; Cohn, R.; Panchapakesan, *Sci. Rep.* **2013**, *3*, 1900, 1.